Biointerface Research in Applied Chemistry
Open-Access Journal (ISSN: 2069-5837)

Article
Volume 13, Issue 3, 2023, 289
https://doi.org/10.33263/BRIAC133.289

Use of Silver Nanoparticles Loaded Locust Bean Gum Coatings to Extend the Shelf-Life of Fruits

Güliz Akyüz [1], Elif Kaymazlar [2], Hilal Ay [3,*], Müberra Andaç [1,2], Ömer Andaç [1,2]

[1] Department of Nanoscience & Nanotechnology, Institute of Graduate Studies, Ondokuz Mayis University, 55200, Kurupelit, Samsun, Turkey; gulz.akyuz@hotmail.com (G.A.); (hilal.ay@omu.edu.tr) (H.A.); mandac@omu.edu.tr (M.A.); oandac@omu.edu.tr (O.A.);
[2] Department of Chemistry, Institute of Graduate Studies, Ondokuz Mayis University, 55200, Kurupelit, Samsun, Turkey; elif.kaymazlar@omu.edu.tr (E.K.); mandac@omu.edu.tr (M.A.); oandac@omu.edu.tr (O.A.);
[3] Department of Molecular Biology and Genetics, Ondokuz Mayis University, 55200, Kurupelit, Samsun, Turkey (hilal.ay@omu.edu.tr) (H.A.);
* Correspondence: gulz.akyuz@hotmail.com (G.A.);

Scopus Author ID 57216587279
Received: 23.05.2022; Accepted: 21.06.2022; Published: 10.07.2022

Abstract: There has been an exponentially increasing concern regarding green synthesis and silver nanoparticles (AgNPs) use in various human contact areas. Here, the synthesis of AgNPs using egg white proteins as alternative antimicrobials and fruit preservation agents was reported. To extend the shelf-life of cherries and apricots was aimed using AgNPs-locust bean gum (LBG) coating. The synthesized nanoparticles were characterized by AAS, Uv-Vis spectroscopy, FTIR, Mastersizer, and SEM/TEM. The amount of the AgNP in the solution was calculated after analyzing silver ion concentration using AAS. SEM, TEM, and Mastersizer results showed the spherical shape of AgNPs with a size distribution from 9 to 13 nm and the hydrodynamic diameter range of 0.1-7 μm, respectively. Their antifungal activities were tested against *Bipolaris sorokiniana*, *Fusarium culmorum*, *Fusarium graminearum*, and *Fusarium verticillioides* using the standard agar well diffusion method. The nanoparticle-based films showed significant inhibition activity against *Bipolaris sorokiniana*-(19 ±2 mm) and *Fusarium graminearum*-(20 ±1 mm). Rotting rate test results showed the synergistic effects of AgNPs and LBG on the shelf life of fruits. Overall, the coating with an AgNPs-LBG solution has the potential use in the fruit industry to extend the shelf life of products.

Keywords: antimicrobials; coatings; fruit preservation, green synthesized; silver nanoparticles.

1. Introduction

Fresh fruit and vegetable consumption has gained much attention due to their significant nutrient source and health benefits in a rapidly growing world. For maintaining quality at the highest standard and extending shelf life, food preservation methods such as antimicrobial applications have become more important [1-4]. Food spoilage can occur through internal and external conditions. Water activity, pH, redox potential, biological components, and all biochemical reactions in the fruit and vegetable can lead to internal spoilage. Fruits and vegetables can be spoiled much faster by external factors such as microbial contamination [5-7].

With increasing attention being paid to the recent advantages of nanotechnological applications, various types of nanoparticles have been evaluated for their antimicrobial features [8-10]. There are many antimicrobial activity studies regarding titanium dioxide [11-14], zinc

oxide [15-17], gold [18-20], and silver nanoparticles [21-23]. However, production methods, toxic chemical composition, and their separation from the synthesis media have great importance for food technology. In this regard, the green synthesis approach of nanoparticles has received great attention. Recently, AgNPs have attracted much interest in food preservation methods because of their special properties such as antineoplastic, antibacterial, antifungal, and antiviral effects. For the synthesis and functionalization of AgNPs, a green synthesis approach could be easily used. Due to green synthesis, toxic chemicals and organic solvents could be eliminated as reducing agents [24-30]. Biologic systems (e.g., microorganisms), many different natural sources, and plant extracts produce AgNPs. For instance, plant extracts, peels, fruits, rhizomes, leaves, or whole plants can be used easily. In the extract, flavonoids, alkaloids, terpenoids, and polyphenols act as reducing agents as well as stabilizing agents. Their reaction with silver ions results in AgNPs [26, 30].

Recently biocompatible polymers such as proteins were chosen for the production of AgNPs. One of them is egg white proteins. Homogeneous and stable sample solutions can be obtained from egg white proteins [31, 32]. Ovalbumin, ovomucoid, ovotransferrin, avidin, lysozyme, ovomucin, ovoflavoprotein, cystatin, ovomacroglobulin, ovoglycoprotein, and ovoinhibitor are the proteins found in egg white [33, 34]. They act as reducing and stabilizing agents for the synthesis of AgNP [31, 32]. Thiyagarajan et al. reported using ovotransferrin, ovalbumin, and ovomucoid as reducing and capping agents for obtaining AgNPs. Also, their antibacterial activity against *Salmonella typhimurium*, and *Escherichia coli* were studied, biocompatibility studies on chicken blood were conducted, and their acute and chronic toxicity was tested on *Drosophila melanogaster* [32]. Also, Owoseni-Fagbenro et al. reported that the egg protein-stabilized AgNPs were synthesized, and the AgNPs were used as an antibiotic (hesperidin) carrier. Their results showed that using AgNPs as a carrier for hesperidin enhanced its therapeutic effectiveness [31]. However, there are limited studies of AgNPs obtained from egg proteins and detail of their inhibitory effect on bacteria and fresh fruit preservation in assays. Also, studies have investigated the synergistic effects of polysaccharides and AgNPs on fruit shelf life. Liang et al. showed the size-controllable preparation of chitosan- AgNP composite microspheres and that small-size chitosan-AgNP composite microspheres could be a promising candidate in the field of antibacterial and fruit preservation applications [35]. Direct application of biodegradable coatings on food surfaces by dipping or spraying can be used to regulate the migration of O_2, CO_2, moisture, lipids, and aroma components. In particular, surface contamination can be inhibited by surface coatings. In recent years, edible films and coatings have attained much interest, and their physical and chemical properties have been broadly investigated [36-39]. Edible coating applications can increase the quality of food. Besides, the nutritional value of food can be protected during storage. Chien et al. studied the effect of a chitosan coating on the quality and shelf life of sliced mango fruit. They found that chitosan coating increased the solid soluble content, titratable acidity, and ascorbic acid content by decreasing water loss and dropping in sensory quality [40]. Generally, edible coatings with good gas and water vapor barrier features are widely investigated [41].

Hydrophilic polymers such as LBG, which contains oxygen and carbon dioxide barrier features, can form viscous solutions at relatively low concentrations. Producing intense edible coatings with good water vapor barrier properties is possible with LBG applications [42]. LBG, also called carob gum, is produced from the fruit of carob trees [43]. It is also a suitable candidate for food packaging material among natural polysaccharides. As side chains, this gum has a β- (1-4) mannopyranose backbone linked to D-galactopyranosyl units [44]. Thanks to its

high viscosity in aqueous solution at low concentrations, biocompatibility, and binding water feature, LBG is used in many food applications as a stabilizer [45], thickening agent [46], and edible film [47]. LBG is stable in a wide range of temperatures and pHs because of its nonionic structure [48]. Also, LBG is affirmed as generally recognized as safe by the United States Food and Drug Administration (FDA). Rojas-Argudo et al. studied the effect of LBG coating on the shelf life of fortune mandarins. They demonstrated that LBG coating improved the external appearance, avoided fruit degradation, and extended shelf life [49].

In this study, we aimed to reveal the effect of antimicrobial LBG coating on the quality and shelf life of apricots and cherries. To our knowledge, the effect of AgNP-loaded LBG coating on the shelf life of apricots and cherries has never been investigated. The main purpose of our study was to develop edible coatings composed of mixtures of AgNPs and LBG and to assess the effect of different ratios of these edible coatings on fruit spoilage processes. Herein, we reported the synthesis of AgNPs via a green synthetic pathway from egg white proteins. The prepared LBG solution was reinforced with synthesized AgNPs. Coating solutions were characterized using Uv-Vis spectra, atomic absorption spectroscopy (AAS), Fourier transform infrared spectroscopy (FTIR), Mastersizer, and scanning/transmission electron microscopy (SEM/TEM) analysis. The antimicrobial properties of the samples on fungi were tested. Lastly, the dip-coating method was chosen for a fruit preservation experiment. Rotting rate assays were conducted for fresh cherries and fresh apricots.

2. Materials and Methods

LBG, $AgNO_3$, and cycloheximide were purchased from Sigma Aldrich. During all the experiments, Millipore water was used (Millipore Applied Systems, USA). Chicken eggs were bought from local markets (Samsun, Turkey). Fresh cherries and apricots were purchased from the local markets (Samsun, Turkey). Fruits with uniformity in size, shape, color, and physical integrity without visual defects were selected. The plant pathogenic fungi strains (*Bipolaris sorokiniana*, *Fusarium culmorum*, *Fusarium graminearum*, and *Fusarium verticillioides*) were obtained from the Department of Plant Protection in Ondokuz Mayis University, Samsun, Turkey.

2.1. Synthesizing of AgNPs via a green synthetic pathway.

The synthesis of AgNPs was studied using a green synthetic pathway according to the previously described procedure [23, 32]. Egg proteins were isolated from fresh chicken eggs. Egg white (EW) was carefully separated from yolk at first. The separated egg white was placed in a clean flask, and almost 27 g of egg white was fully dissolved in 200 mL distilled water with a strong magnetic stirrer (300 rpm) for 60 minutes. The mixture of various proteins in egg white is mostly soluble in distilled water.

The cloudy white solution was observed and filtered through Whatman filter paper. The clear solution was stored at 4°C until required for further analysis. The clear egg white solution (1 mL) was mixed with 1 mM of (respectively 4, 6, and 8 mL) $AgNO_3$ solution at room temperature. The reaction mixture showed a color change from white to dark yellow with time. To determine the maximum nanoparticle formation, samples were collected at different time intervals (i.e., 24, 48, 72, and 96 hours) and analyzed using AAS, FTIR spectroscopy, Uv-Vis spectroscopy, Mastersizer, and SEM/TEM.

2.2. Preparation of LBG-AgNP composite microspheres.

The LBG-AgNP solution was prepared using a slightly modified version of a method in a previous study [50]. LBG solutions (1% and 1.5%) were prepared in water at 60°C under magnetic stirring (300 rpm) overnight. The obtained LBG solutions were added to the synthesized AgNPs solution under magnetic stirring (300 rpm), and the mixture was stirred for almost 6 hours to form a homogeneous solution. Finally, the homogeneous solution that eventually formed was kept at 4°C for further applications.

2.3. Characterization.

Samples were characterized using a Uv-Vis spectrophotometer (Thermo fisher scientific, G10S), and distilled water was used as a blank. Uv-Vis spectroscopic analysis was studied by scanning at a range of 190-900 nm. A color change was observed in the reduction of silver ions to AgNPs by egg white proteins. The color of the $AgNO_3$/egg white proteins' extract mixture changed from white to dark yellow due to the formation of AgNPs. The detection approved the formation of the AgNPs of the surface plasmon resonance (SPR) absorption band between 400 nm and 475 nm in the Uv-Vis spectrum. The samples' FTIR spectra (PerkinElmer, Spectrum two, USA) were recorded using an infrared spectrometer to characterize the interaction between the AgNPs and protein present in the egg white. EW-AgNPs were recorded in a range of 400-4000 cm^{-1} using the spectrometer. The samples' surface morphology and particle sizes were observed using SEM (JEOL-JSM-7001F). Transmission electron microscopy (TEM) images were obtained on a JEOL-JSM 7001F using a STEM detector with an accelerating voltage of 30 kV. The particle sizes were calculated using the ImageJ software [51]. The amount of AgNPs in the solutions was calculated after analyzing silver ion concentration using the Perkin Elmer PinAAcle 900f Atomic Absorption Spectrometer (AAS) mounted with a silver hollow cathode lamp (Photron). Silver standards of 0.125 ppm, 0.25 ppm, 0.50 ppm, 0.75 ppm, and 1.00 ppm have been prepared and used to obtain a calibration curve with an $R^2 = 0.9992$. After synthesizing of AgNPs, the solutions were centrifuged, and then the supernatants were analyzed using AAS. The concentrations of silver ions in the supernatants were calculated using a calibration curve. The concentrations of AgNPs in the solutions were calculated by subtracting the initial concentration of silver ions by the concentration of silver ions in the supernatants. The particle size of AgNPs was analyzed using a Mastersizer Hydro 3000. Measurements were performed in the range between 0.01 and 1000 µm with the particle refractive index (n: 0.135), particle absorption coefficient (k: 3.99), and particle bulk density (0.312 g/cm^3).

2.4. Antifungal activity tests.

The plant pathogenic fungi strains (*Bipolaris sorokiniana*, *Fusarium culmorum*, *Fusarium graminearum*, and *Fusarium verticillioides*) were obtained from the Department of Plant Protection in Ondokuz Mayis University, Samsun, Turkey. The antifungal activity of synthesized nanoparticles was determined using agar well diffusion as described by Magaldi et al. [52]. The fungi were grown in potato dextrose broth for 48 hours before inoculation onto potato dextrose agar (PDA) medium. An aliquot of 200 µL of each strain was spread onto the PDA medium and then allowed to dry under aseptic conditions. The wells were made using a cork borer and filled with 100 µL of nanoparticle solutions prepared in different concentrations. Cycloheximide (25 µg/mL) was used as the positive control, while egg white and silver nitrate

were used as negative controls. After incubation for 2 days at 35±1°C, the zone of inhibitions was measured.

2.5. Rotting rate assay.

Fresh cherries and apricots (purchased from a local market, Samsun, Turkey) with a moderate size were selected and washed with distilled water, then dried at room temperature. Dip coating was used on the fruits, and each group was placed on a clean plate. Then, the plates were wrapped in polyethylene film and stored at a constant temperature of 25±1°C. Changes in the fruits were observed and the data collected, and images were taken every 24 h. Mold and rotting conditions were observed. The rotting rate was calculated using the following Eq (1) [53]:

$$\text{Rotting Rate (\%)} = (x_t / x_0) * 100\% \quad (1)$$

x_0: the total number of samples
x_t: the number of rotting after a storage time t (d).

3. Results and Discussion

3.1. Green synthesis of AgNPs.

Nowadays, the green synthesis of metallic nanoparticles has garnered greater attraction than chemically produced ones. Green plants, microorganisms, and polymers are used for the green production of AgNPs [54-57]. Egg white proteins were used as reduction agents to obtain AgNPs (Table 1). Compounds with thiol (-SH) groups (such as cysteine) present in protein molecules reduce Ag^+ ions to form spherical AgNPs [31, 58]. It has been proven that Ag^+ reacts with proteins by binding with hydroxyl (-OH), carboxyl (-COOH), an amine (N-H) groups and acts as a reduction agent for Ag^+ [31, 59]. The egg white protein function as a reducing agent in the green synthesis of AgNPs is shown in Figure 1.

Table 1. Prepared samples from egg white proteins for an antimicrobial test.

Egg White Protein Solution (mL)		**1 mM $AgNO_3$ Solution (mL)**
EW1/4	1	4
EW1/6	1	6
EW1/8	1	8

AgNPs absorption peaks were observed up to 96 h (Figure 2). The solutions showed a color change from white to dark brown due to the reduction of Ag^+ into Ag^0. The intensity of the peaks at 350-600 nm increases up to 72 h, shown in Figure 2. This means that the concentration of the AgNPs is shown in a gradual increase of surface plasmon resonance (SPR) peak intensity for 72 h, but peak intensity decreases for 96 h (Figure 2). Therefore, the absorption completely depends on the chemical surroundings, particle size, and dielectric medium, which demonstrates that it is an efficient method for observing the electron injection and aggregation of nanoparticles [60]. Furthermore, enhancing the nanoparticle size and forming an aggregation of nanoparticles can cause a sensible broadening of the plasmonic band towards larger wavelengths [60-62]. The maximum intensity of the absorption peak was observed in the EW1/4, EW1/6, and EW1/8 for 72 h, and these solutions were used for further studies.

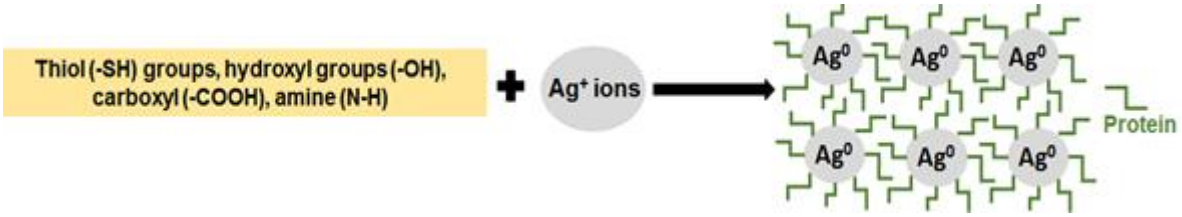

Figure 1. Green synthesis of AgNPs.

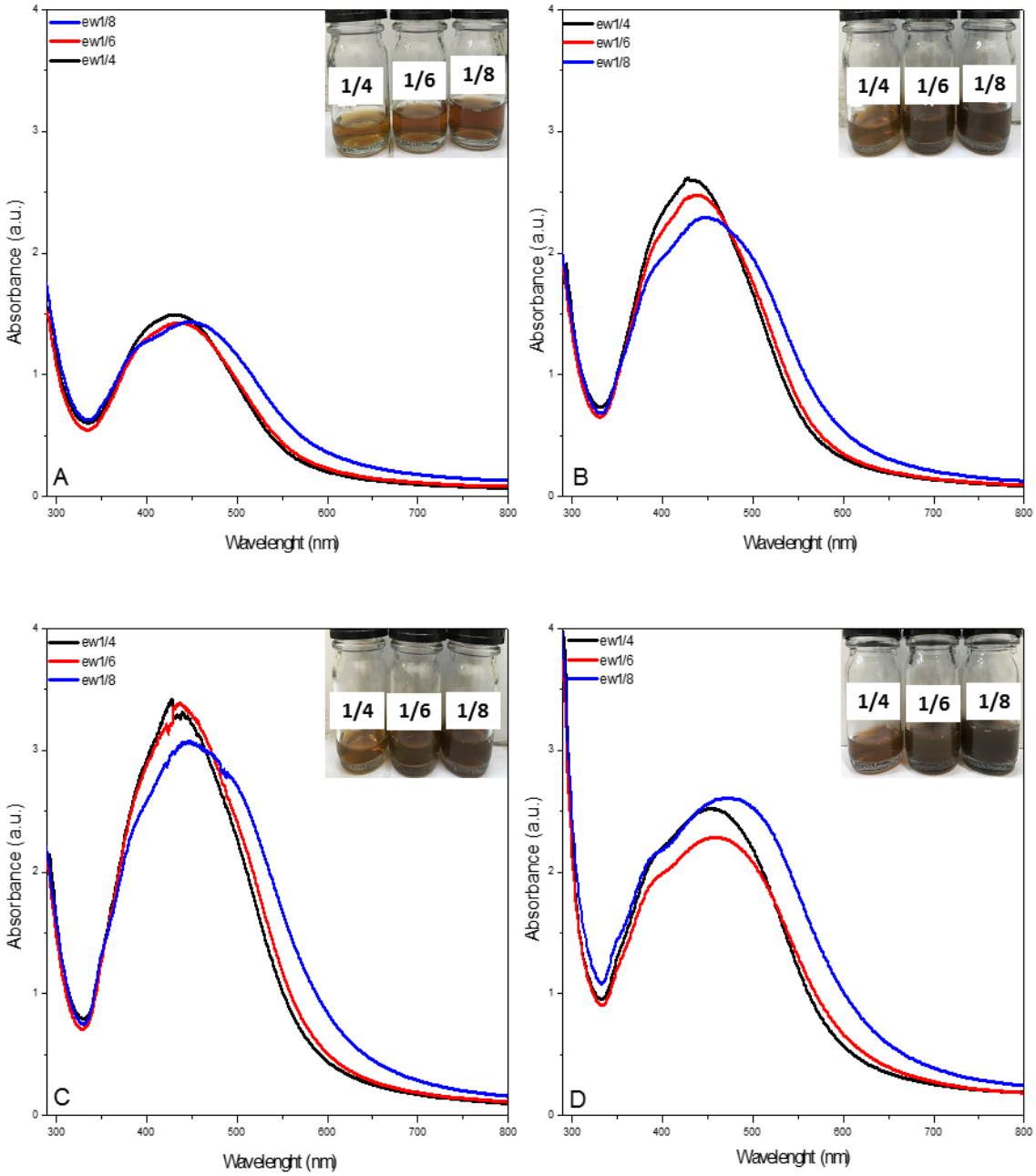

Figure 2. Uv-vis spectroscopy results of the green synthesized AgNPs after (**A**) 24 hours; (**B**) 48 hours; (**C**) 72 hours; (**D**) 96 hours.

3.2. Fourier-transform infrared (FTIR) spectroscopy.

The FTIR spectra of the samples are shown in Figure 3. Ovalbumin (54%), ovotransferrin (12%), ovomucoid (11%), ovomucin (3.5%), and lysozyme (3.5%) are among the major egg white proteins [34]. The amine, thiol, carboxyl, and hydroxyl groups of egg white proteins can donate electrons to reduce Ag+ to Ag0 and stabilize nanoparticles [31]. The strong

peak at around 3270 cm^{-1} was assigned to –OH stretching of the proteins in the egg white. The spectra reveal amide I (1620 cm^{-1}) and amide II (1525 cm^{-1}) bands due to the bending vibrations of the C=O and N-H bonds in the amide of the proteins, respectively [63]. The peak at 2970 cm^{-1} could be assigned to the C-H stretching vibration of the methyl, methylene, and methoxy groups. The new peak at 1740 cm^{-1} could be assigned to aldehyde or ketone groups that were oxidized after the reduction of silver ions. These results indicated that egg white proteins acted both as a reducing agent and capping agent for AgNPs.

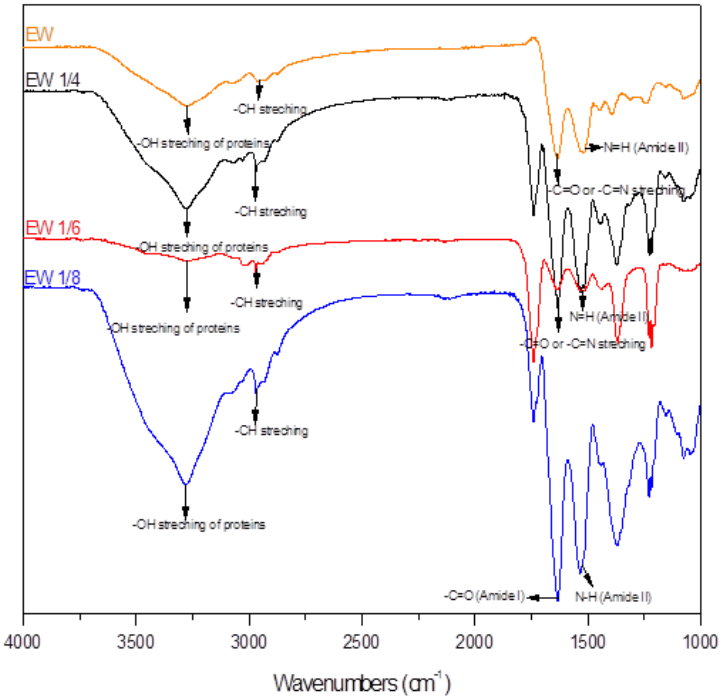

Figure 3. FTIR spectra of the nanoparticle solutions.

3.3. AAS.

The concentrations of AgNPs in the solutions and percentage conversion of silver ions to AgNPs were determined using AAS. The results are given in Table 2. As seen in Table 2, the conversion of the silver ions to AgNPs increased with the concentration of silver ions in the biomass. The highest AgNPs concentration was found as EW 1/8 with 40% conversion.

Table 2. AAS results of the samples.

	C_{Ag^+} (initial) (mg/L)	C_{Ag^+} (supernatant) (mg/L)	C_{AgNPs} (mg/L)	AgNPs (%)
EW1/4	0.6048	0.5557	0.0491	8.111
EW1/6	0.6480	0.4383	0.2096	32.35
EW1/8	0.6720	0.4029	0.2691	40.05

3.4. Mastersizer.

The samples' particle size and size distribution were investigated using sizes ranging from 0.1 to 1000 nm using laser diffractometry (Figure 4). Measurements were taken in the range between 0.01 and 1000 μm with the particle refractive index (n: 0.135), particle absorption coefficient (k: 3.99), and particle bulk density (0.312 g/cm^3). The average hydrodynamic diameter of the particles of EW1/6 and EW1/8 is 0.2 μm, and the volume distributions are 3.6% and 6.8%, respectively. The average hydrodynamic diameter of EW1/4

is 7 μm, and the volume distribution is 2.7%. EW1/4 shows broader particle distribution compared with EW1/6 and EW1/8.

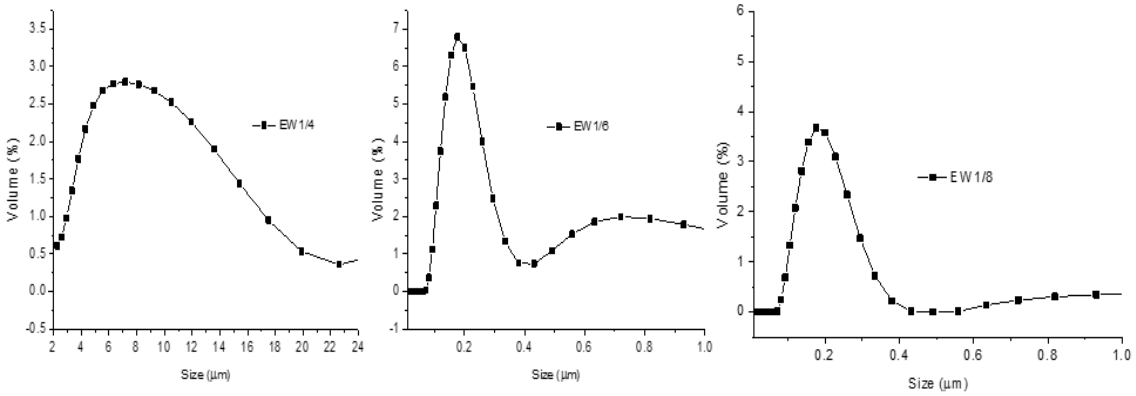

Figure 4. Particle size distribution of green synthesized AgNPs.

3.5. SEM/TEM Analysis.

The size and morphology of the egg white-capped AgNPs were measured using SEM. Powder samples were attached to the carbon band. When the morphology of AgNP is examined, AgNPs are spherical, and their size is below 50 nm (Figure 5). Respectively, 4 mL, 6 mL, and 8 mL of LBG 1% and LBG 1.5% solutions were added to the samples of EW1/4, EW1/6, and EW1/8. Their SEM images are shown in Figure 5.

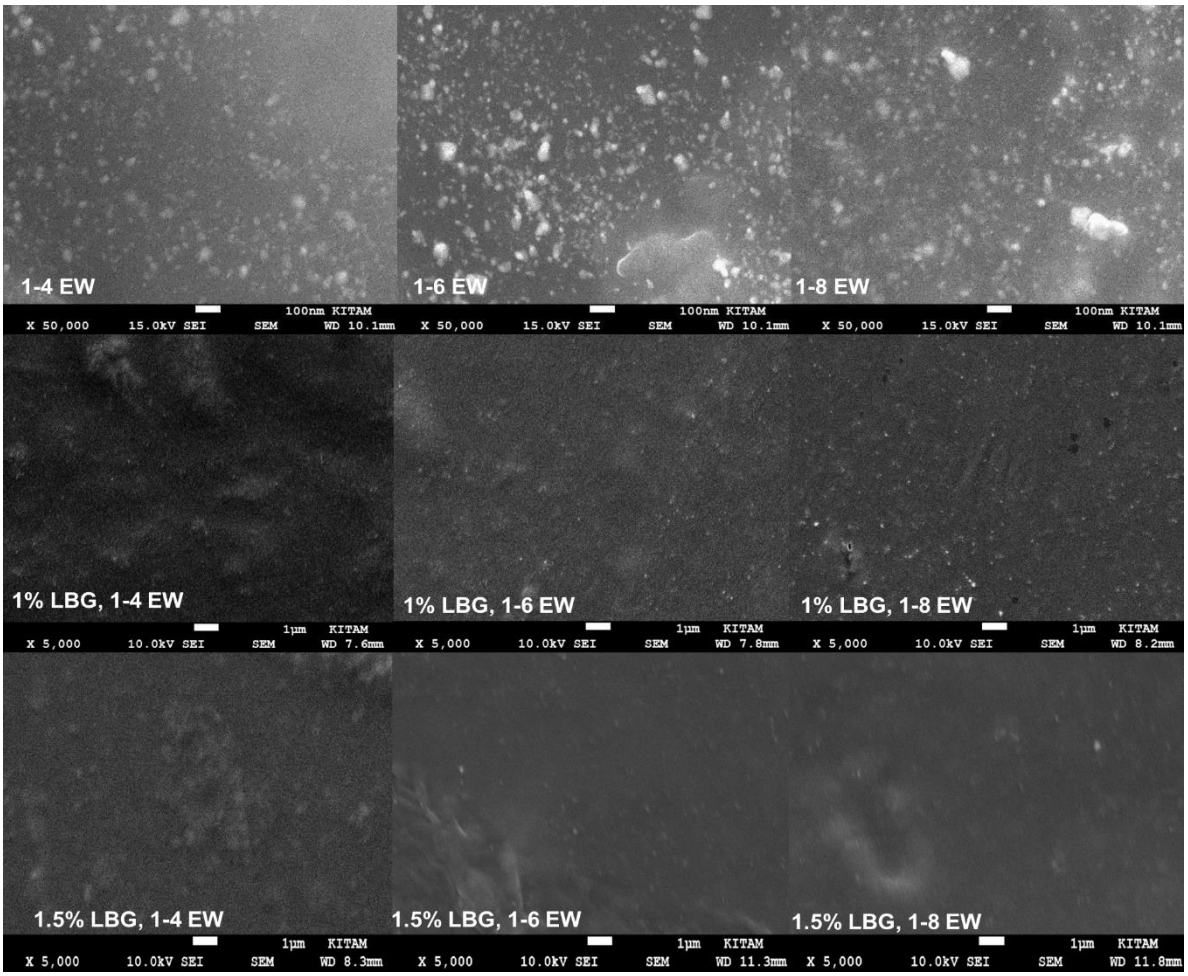

Figure 5. SEM image of the green synthesized AgNPs for EW1/4, EW1/6, EW1/8, and different ratios of EW-LBG.

The TEM images and particle size distributions of the AgNPs are given in Figure 6. The images reveal spherical shapes and uniform distributions of nanoparticles. The average particle size ranges of the nanoparticles were between 9-13 nm, as shown in Figure 6. It is seen from TEM results that the particle size increased with the increase of initial silver ion concentration. TEM images of EW1/8 show slightly larger nanoparticles. It was likely due to the high initial silver ion concentration causing aggregation.

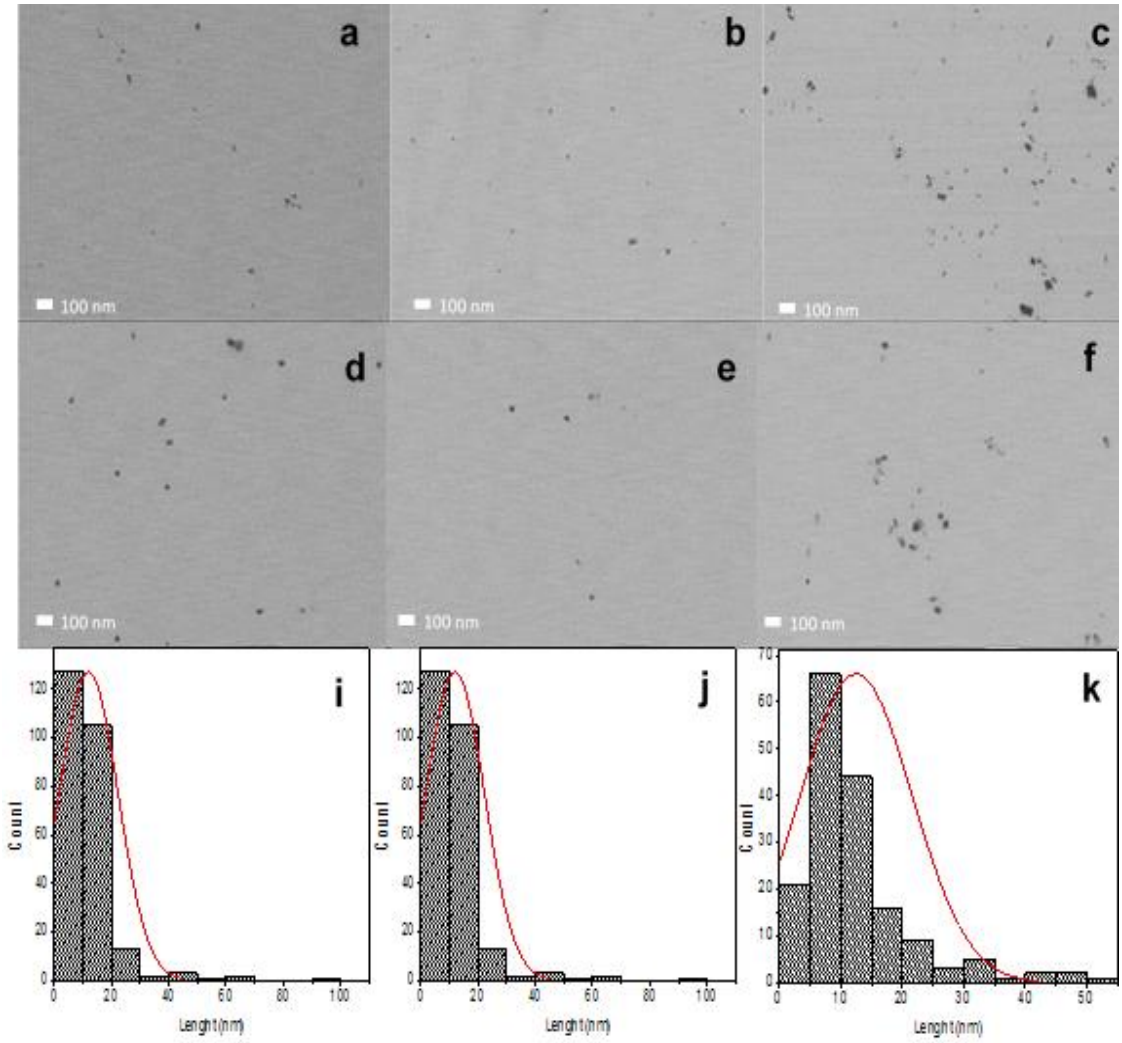

Figure 6. TEM images and particle size distributions of the samples (a,d,i) EW1/4, (b,e,j) EW1/6 and (c,f,k) EW1/8.

3.6. Antifungal activity test results.

The antimicrobial efficacy of AgNPs depends on many factors. AgNPs can attach to the microorganism cell wall and easily pass through it. Due to this phenomenon, cell membranes could be damaged, and cytoplasm content can leak. AgNPs could interact with vital cellular structures and biomolecules such as DNA. Besides, they can affect ATP synthesis mechanisms. They might cause cell apoptosis due to DNA damage, lipid peroxidation, and increased reactive oxygen species [27, 64]. In this study, the antifungal activities of the synthesized nanoparticles were tested against *Bipolaris sorokiniana*, *Fusarium culmorum*, *Fusarium graminearum*, and *Fusarium verticillioides*, which are causative agents of several plant diseases such as common root rot, leaf spot disease, seedling blight, head blight, and black point of cereals [65, 66]. AgNPs showed significant inhibitory activity against *Bipolaris*

sorokiniana and *Fusarium graminearum*, but they were not effective against *Fusarium culmorum* and *Fusarium verticillioides* (Table 3).

Table 3. Antifungal activity of AgNPs, coating solutions, and control groups.

	Inhibition zone (mm)			
Sample	***B. sorokiniana***	***F. culmorum***	***F. graminearum***	***F. verticillioides***
EW 1/4	10 ±0 mm	6 ±0 mm	17 ±1 mm	6 ±0 mm
EW 1/6	17 ±1 mm	6 ±0 mm	19 ±2 mm	6 ±0 mm
EW 1/8	15 ±3 mm	6 ±0 mm	20 ±2 mm	6 ±0 mm
EW 1/4 + 1 % LBG	18 ±1 mm	6 ±0 mm	20 ±1 mm	6 ±0 mm
EW 1/6 + 1 % LBG	18 ±1 mm	6 ±0 mm	14 ±1 mm	6 ±0 mm
EW 1/8 + 1 % LBG	19 ±1 mm	6 ±0 mm	18 ±3 mm	6 ±0 mm
EW 1/4 + 1.5 % LBG	15 ±3 mm	6 ±0 mm	15 ±1 mm	6 ±0 mm
EW 1/6 + 1.5 % LBG	18 ±1 mm	6 ±0 mm	18 ±1 mm	6 ±0 mm
EW 1/8 + 1.5 % LBG	19 ±2 mm	6 ±0 mm	19 ±1 mm	6 ±0 mm
1 % LBG	9 ±1 mm	8 ±1 mm	7 ±1 mm	8 ±1 mm
1.5 % LBG	8 ±0 mm	8 ±1 mm	8 ±1 mm	8 ±1 mm
EW	9 ±0 mm	9 ±1 mm	9 ±1 mm	9 ±1 mm
$AgNO_3$	9 ±0 mm	9 ±1 mm	9 ±1 mm	9 ±1 mm
Cycloheximide(25 µg/ml)	31 ±1 mm	41 ±3 mm	31 ±1 mm	41 ±2 mm

3.7. Rotting rate test results.

After dip coating treatments, the antimicrobial activity of fruit samples was studied using the rotting rate. The appearance of the fruits during the storage period is shown in Figure 7. The rotting rate of all samples increased progressively throughout the storage time, as shown in Figure 8 and Figure 9. The degradation of fruits was more significant in the blank fruits and just LBG-added samples. The usage of AgNPs considerably decreased the rotting rate with the dip-coating method.

The synergistic effects of AgNPs and LBG on the shelf life of fruits were observed. LBG-AgNPs solutions showed better results for both apricots and cherries. Also, only LBG-coated apricots became 100% rotten on the fourth day due to LBG possessing good oxygen and carbon dioxide barrier features, whereas it is a hydrophilic polymer. The appearance of apricots showed a significant difference from the 10th day (Figure 7). On the fifth day, most apricots in the blank group were rotten, whereas the coated apricots showed no considerable difference on their surface until the 10th day, except for 1/4EW- LBG 1%. Also, cherries in the blank group were rotten on the fourth day, and only LBG-coated cherries were rotten on the fifth day (Figure 7). Food spoilage is an unacceptable process for healthy consumption.

Generally, fresh fruits possess beneficial conditions for microbiologic resistance. Microbial spoilage can affect fruits and fruit juices much quicker than the variety of intrinsic conditions of the fruit [67, 68]. Also, water activity, pH, redox potential, biologic components, and all biochemical reactions in the fruit lead to its spoilage in different ways [5-7]. As observed, cherries have more survival conditions than apricots in the same experimental conditions. Apricots are more perishable fruits.

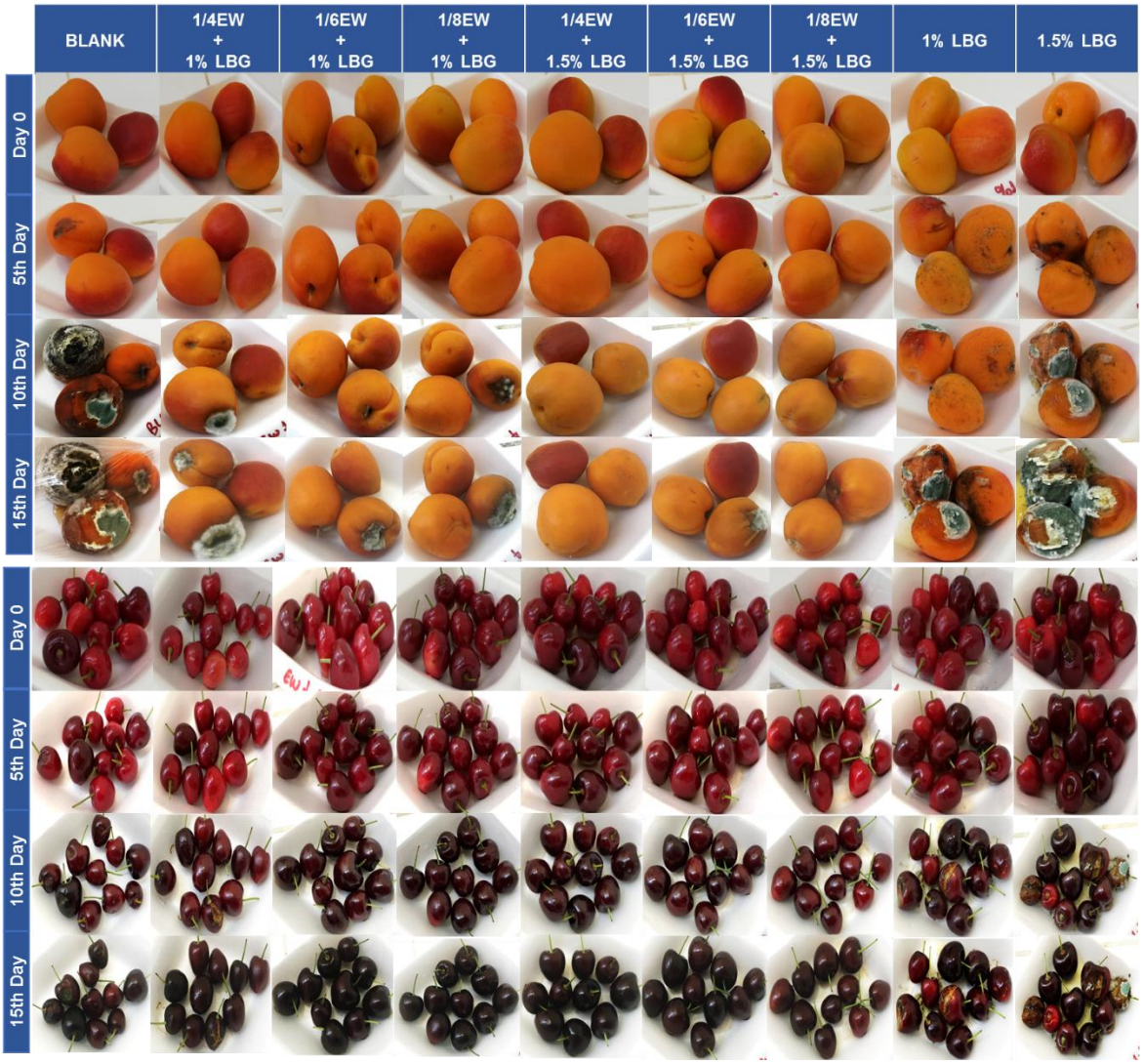

Figure 7. Change of appearance of apricots and cherries during storage.

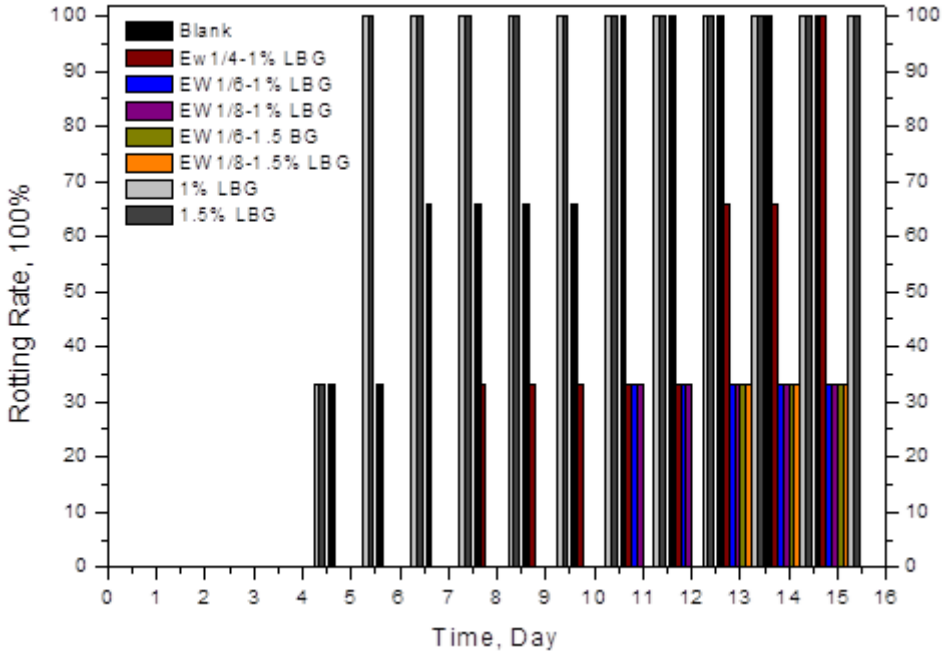

Figure 8. Rotting rate of apricots within one week.

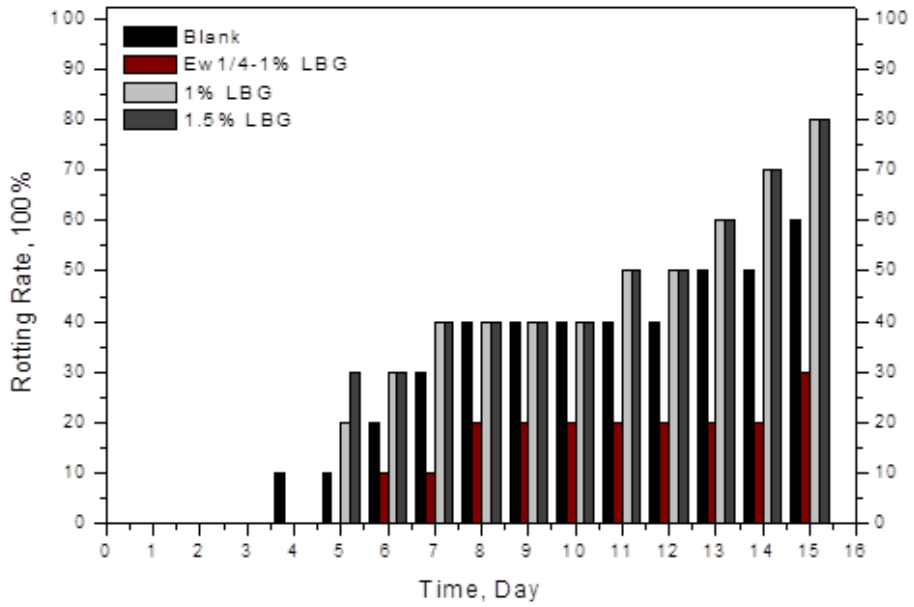

Figure 9. Rotting rate of cherries among one month.

4. Conclusions

The green chemistry method was used to synthesize AgNPs from silver nitrate solution using egg white proteins at room temperature. Then, LBG solutions were obtained, and it was reinforced with the prepared AgNP solution. Uv-Vis spectroscopy, FTIR, SEM, TEM, AAS, and master size analyses were studied for the characterization of the samples. The maximum surface plasmon resonance bands were observed in the Uv-Vis spectrum for the samples at 72 hours. Also, the FTIR results showed that egg white proteins acted as both reducing and capping agents for AgNPs synthesis. The size distribution of AgNPs was found between 9 and 13 nm, according to the TEM results. Atomic absorption spectroscopy results showed that the concentration of the AgNPs in the EW1/4, EW1/6, and EW1/8 solutions were respectively 0.0491 mg/L, 0.2096 mg/L, and 0.2691 mg/L.

Further, the antifungal performance of the synthesized AgNPs and AgNP – LBG solutions were examined against plant pathogenic fungi, *Bipolaris sorokiniana*, *Fusarium culmorum*, *Fusarium graminearum*, and *Fusarium verticillioides*. The AgNPs notably inhibited the growth of *Bipolaris sorokiniana* and *Fusarium graminearum*. Additionally, the dip-coating treatment was applied to the fresh fruits. The antimicrobial activities of the AgNP and AgNP – LBG samples on the fresh fruits were observed. The rotting rate showed the coatings' good antimicrobial properties on the fresh fruits. The results showed that the AgNP and AgNP – LBG samples possess a strong antifungal effect as coatings. Also, the coating treatment supported the shelf life of the cherries and the apricots. The rotting rate of fruits was more significant in the LBG - only samples, but it was considerably decreased with AgNPs with dip coating. AgNPs reinforced solutions showed better results for both the apricots and the cherries. LBG – AgNP nanocomposites incorporated as coatings can extend the shelf-life of fresh apricots and fresh cherries. The prepared coating agents have great potential as alternative food preservatives in the fresh fruit industry. AgNPs are promising antifungal agents, and our results will lead to the exploration of novel antimicrobial applications in the fruit industry.

Funding

This research received no external funding.

Acknowledgments

This research work was supported as a part of a BAP research project at the Ondokuz Mayis University (Project Number: PYO.FEN.1901.18.008).

Conflicts of Interest

The authors declare no conflict of interest.

References

1. Khodijah Chaerun, S.; Akbar Prabowo, B.; Winarko, R. Bionanotechnology: the formation of copper nanoparticles assisted by biological agents and their applications as antimicrobial and antiviral agents. *Environmental Nanotechnology, Monitoring & Management* **2022**, *18*, 100703, https://doi.org/10.1016/j.enmm.2022.100703.
2. Bahrami, A.; Delshadi, R.; Cacciotti, I. et al. Targeting foodborne pathogens via surface-functionalized nano-antimicrobials. *Adv Colloid Interface Sci* **2022**, *302*, 102622, https://doi.org/10.1016/j.cis.2022.102622.
3. Truong, V.K.; Al Kobaisi, M.; Vasilev, K.; Cozzolino, D.; Chapman, J. Current Perspectives for Engineering Antimicrobial Nanostructured Materials. *Current Opinion in Biomedical Engineering* **2022**, *23*, 100399, https://doi.org/10.1016/j.cobme.2022.100399.
4. Saleemi, M.A.; Lim, V. Overview of antimicrobial polyurethane-based nanocomposite materials and associated signalling pathways. *European Polymer Journal* **2022**, *167*, 111087, https://doi.org/10.1016/j.eurpolymj.2022.111087.
5. Alwazeer, D. Importance of consideration of oxidoreduction potential as a critical quality parameter in food industries. *Food Research International* **2020**, *132*, 109108, https://doi.org/10.1016/j.foodres.2020.109108.
6. Gao, T.; Tian, Y.; Zhu, Z.; Sun, D.-W. Modelling, responses and applications of time-temperature indicators (TTIs) in monitoring fresh food quality. *Trends in Food Science & Technology* **2020**, *99*, 311-322, https://doi.org/10.1016/j.tifs.2020.02.019.
7. Jiang, S.; Liu, Y. Gas sensors for volatile compounds analysis in muscle foods: A review. *TrAC Trends in Analytical Chemistry* **2020**, *126*, 115877, https://doi.org/10.1016/j.trac.2020.115877.
8. Cao, Y.; Naseri, M.; He, Y.; Xu, C.; Walsh, L.J.; Ziora, Z.M. Non-antibiotic Antimicrobial Agents to Combat Biofilm-forming Bacteria. *J Glob Antimicrob Resist* **2020**, *21*, 445-451, https://doi.org/10.1016/j.jgar.2019.11.012.
9. Youssef, A.M.; El-Sayed, S.M. Bionanocomposites materials for food packaging applications: Concepts and future outlook. *Carbohydr Polym* **2018**, *193*, 19-27, https://doi.org/10.1016/j.carbpol.2018.03.088.
10. Matatkova, O.; Michailidu, J.; Miskovska, A.; Kolouchova, I.; Masak, J.; Cejkova, A. Antimicrobial properties and applications of metal nanoparticles biosynthesized by green methods. *Biotechnol Adv* **2022**, *58*, 107905, https://doi.org/10.1016/j.biotechadv.2022.107905.
11. Lee, S.-Y.; Park, S.-J. TiO_2 photocatalyst for water treatment applications. *Journal of Industrial and Engineering Chemistry* **2013**, *19*, 1761-1769, https://doi.org/10.1016/j.jiec.2013.07.012.
12. Rodríguez-González, V.; Obregón, S.; Patrón-Soberano, O.A.; Terashima, C.; Fujishima, A. An approach to the photocatalytic mechanism in the TiO2-nanomaterials microorganism interface for the control of infectious processes. *Applied Catalysis B: Environmental* **2020**, *270*, 118853, https://doi.org/10.1016/j.apcatb.2020.118853.
13. Uyguner Demirel, C.S.; Birben, N.C.; Bekbolet, M. A comprehensive review on the use of second generation TiO2 photocatalysts: Microorganism inactivation. *Chemosphere* **2018**, *211*, 420-448, https://doi.org/10.1016/j.chemosphere.2018.07.121.
14. Anbumani, D.; Dhandapani, K.v.; Manoharan, J.; Babujanarthanam, R.; Bashir, A.K.H.; Muthusamy, K.; Alfarhan, A.; Kanimozhi, K. Green synthesis and antimicrobial efficacy of titanium dioxide nanoparticles using Luffa acutangula leaf extract. *Journal of King Saud University - Science* **2022**, *34*, 101896, https://doi.org/10.1016/j.jksus.2022.101896.

15. Mani, V.M.; Nivetha, S.; Sabarathinam, S.; Barath, S.; Das, M.P.A.; Basha, S.; Elfasakhany, A.; Pugazhendhi, A. Multifunctionalities of mycosynthesized zinc oxide nanoparticles (ZnONPs) from *Cladosporium tenuissimum* FCBGr: Antimicrobial additives for paints coating, functionalized fabrics and biomedical properties. *Progress in Organic Coatings* **2022**, *163*, 106650, https://doi.org/10.1016/j.porgcoat.2021.106650.
16. Mallikarjunaswamy, C.; Vidya, J.S.; Deepakumari, H.N.; Nagaraju, G.; Sangamesha, M.A.; Lakshmi Ranganatha, V. Larvicidal and antimicrobial activity of zinc oxide nanoparticles synthesized from rain tree pod aqueous extract. *Materials Today: Proceedings* **2022**, *62*, 5083-5086, https://doi.org/10.1016/j.matpr.2022.02.422.
17. Sharma, P.; Urfan, M.; Anand, R.; Sangral, M.; Hakla, H.R.; Sharma, S.; Das, R.; Pal, S.; Bhagat, M. Green synthesis of zinc oxide nanoparticles using Eucalyptus lanceolata leaf litter: characterization, antimicrobial and agricultural efficacy in maize. *Physiol Mol Biol Plants* **2022**, *28*, 363-381, https://doi.org/10.1007/s12298-022-01136-0.
18. Ramalingam, V. Multifunctionality of gold nanoparticles: Plausible and convincing properties. *Adv Colloid Interface Sci* **2019**, *271*, 101989, https://doi.org/10.1016/j.cis.2019.101989.
19. Pawar, C.A.; Sharma, A.K.; Prasad, N.R.; Suryawanshi, S.S.; Nazeruddin, G.M.; Shaikh, V.S.; Kulkarni, A.N.; Al-Sehemi, A.G.; Shaikh, Y.I. A comparative study on antimicrobial efficacies of biologically synthesized nano gold using *Bos taurus indicus* urine with pharmaceutical drug sample. *Current Research in Green and Sustainable Chemistry* **2022**, *5*, 100311, https://doi.org/10.1016/j.crgsc.2022.100311.
20. Gnanamoorthy, G.; Ramar, K.; Ali, D.; Yadav, V.K.; Jafar ahamed, A.; Kumar, G. Synthesis and effective performance of Photocatalytic and Antimicrobial activities of Bauhinia tomentosa Linn plants using of gold nanoparticles. *Optical Materials* **2022**, *123*, 111945, https://doi.org/10.1016/j.optmat.2021.111945.
21. Deshmukh, S.P.; Patil, S.M.; Mullani, S.B.; Delekar, S.D. Silver nanoparticles as an effective disinfectant: A review. *Mater Sci Eng C Mater Biol Appl* **2019**, *97*, 954-965, https://doi.org/10.1016/j.msec.2018.12.102.
22. Tortella, G.R.; Rubilar, O.; Duran, N.; Diez, M.C.; Martinez, M.; Parada, J.; Seabra, A.B. Silver nanoparticles: Toxicity in model organisms as an overview of its hazard for human health and the environment. *J Hazard Mater* **2020**, *390*, 121974, https://doi.org/10.1016/j.jhazmat.2019.121974.
23. Matar, G.H.; Akyüz, G.; Kaymazlar, E.; Andac, M. An Investigation of Green Synthesis of Silver Nanoparticles Using Turkish Honey Against Pathogenic Bacterial Strains. *Biointerface Research in Applied Chemistry* **2022**, *13*, 195, https://doi.org/10.33263/BRIAC132.195.
24. Arumai Selvan, D.; Mahendiran, D.; Senthil Kumar, R.; Kalilur Rahiman, A. Garlic, green tea and turmeric extracts-mediated green synthesis of silver nanoparticles: Phytochemical, antioxidant and in vitro cytotoxicity studies. *J Photochem Photobiol B* **2018**, *180*, 243-252, https://doi.org/10.1016/j.jphotobiol.2018.02.014.
25. Escarcega-Gonzalez, C.E.; Garza-Cervantes, J.A.; Vazquez-Rodriguez, A. et al. In vivo antimicrobial activity of silver nanoparticles produced via a green chemistry synthesis using Acacia rigidula as a reducing and capping agent. *Int J Nanomedicine* **2018**, *13*, 2349-2363, https://doi.org/10.2147/ijn.s160605.
26. Rolim, W.R.; Pelegrino, M.T.; de Araújo Lima, B.; Ferraz, L.S.; Costa, F.N.; Bernardes, J.S.; Rodigues, T.; Brocchi, M.; Seabra, A.B. Green tea extract mediated biogenic synthesis of silver nanoparticles: Characterization, cytotoxicity evaluation and antibacterial activity. *Applied Surface Science* **2019**, *463*, 66-74, https://doi.org/10.1016/j.apsusc.2018.08.203.
27. Saxena, V.; Chandra, P.; Pandey, L.M. Design and characterization of novel Al-doped ZnO nanoassembly as an effective nanoantibiotic. *Applied Nanoscience* **2018**, *8*, 1925-1941, https://doi.org/10.1007/s13204-018-0863-0.
28. Sharma, V.K.; Yngard, R.A.; Lin, Y. Silver nanoparticles: green synthesis and their antimicrobial activities. *Adv Colloid Interface Sci* **2009**, *145*, 83-96, https://doi.org/10.1016/j.cis.2008.09.002.
29. Suarez-Cerda, J.; Nunez, G.A.; Espinoza-Gomez, H.; Flores-Lopez, L.Z. A comparative study of the effect of alpha-, beta-, and gamma-cyclodextrins as stabilizing agents in the synthesis of silver nanoparticles using a green chemistry method. *Mater Sci Eng C Mater Biol Appl* **2014**, *43*, 21-26, https://doi.org/10.1016/j.msec.2014.07.006.
30. Zia, F.; Ghafoor, N.; Iqbal, M.; Mehboob, S. Green synthesis and characterization of silver nanoparticles using *Cydonia oblong* seed extract. *Applied Nanoscience* **2016**, *6*, 1023-1029, https://doi.org/10.1007/s13204-016-0517-z.
31. Owoseni-Fagbenro, K.A.; Saifullah, S.; Imran, M. et al. Egg proteins stabilized green silver nanoparticles as delivery system for hesperidin enhanced bactericidal potential against resistant S. aureus. *Journal of Drug Delivery Science and Technology* **2019**, *50*, 347-354, https://doi.org/10.1016/j.jddst.2019.02.002.

32. Thiyagarajan, K.; Bharti, V.K.; Tyagi, S.; Tyagi, P.K.; Ahuja, A.; Kumar, K.; Raj, T.; Kumar, B. Retracted article: Synthesis of non-toxic, biocompatible, and colloidal stable silver nanoparticle using egg-white protein as capping and reducing agents for sustainable antibacterial application. *RSC Advances* **2018**, *8*, 23213-23229, https://doi.org/10.1039/C8RA03649G.
33. Abeyrathne, E.; Huang, X.; Ahn, D.U. Antioxidant, angiotensin-converting enzyme inhibitory activity and other functional properties of egg white proteins and their derived peptides - A review. *Poult Sci* **2018**, *97*, 1462-1468, https://doi.org/10.3382/ps/pex399.
34. Abeyrathne, E.D.; Lee, H.Y.; Ahn, D.U. Egg white proteins and their potential use in food processing or as nutraceutical and pharmaceutical agents--a review. *Poult Sci* **2013**, *92*, 3292-3299, https://doi.org/10.3382/ps.2013-03391.
35. Liang, J.; Wang, J.; Li, S.; Xu, L.; Wang, R.; Chen, R.; Sun, Y. The size-controllable preparation of chitosan/silver nanoparticle composite microsphere and its antimicrobial performance. *Carbohydr Polym* **2019**, *220*, 22-29, https://doi.org/10.1016/j.carbpol.2019.05.048.
36. Carbone, M.; Donia, D.T.; Sabbatella, G.; Antiochia, R. Silver nanoparticles in polymeric matrices for fresh food packaging. *Journal of King Saud University - Science* **2016**, *28*, 273-279, https://doi.org/10.1016/j.jksus.2016.05.004.
37. Maringgal, B.; Hashim, N.; Mohamed Amin Tawakkal, I.S.; Muda Mohamed, M.T. Recent advance in edible coating and its effect on fresh/fresh-cut fruits quality. *Trends in Food Science & Technology* **2020**, *96*, 253-267, https://doi.org/10.1016/j.tifs.2019.12.024.
38. Umaraw, P.; Munekata, P.E.S.; Verma, A.K.; Barba, F.J.; Singh, V.P.; Kumar, P.; Lorenzo, J.M. Edible films/coating with tailored properties for active packaging of meat, fish and derived products. *Trends in Food Science & Technology* **2020**, *98*, 10-24, https://doi.org/10.1016/j.tifs.2020.01.032.
39. Yousuf, B.; Qadri, O.S.; Srivastava, A.K. Recent developments in shelf-life extension of fresh-cut fruits and vegetables by application of different edible coatings: A review. *LWT* **2018**, *89*, 198-209, https://doi.org/10.1016/j.lwt.2017.10.051.
40. Chien, P.-J.; Sheu, F.; Yang, F.-H. Effects of edible chitosan coating on quality and shelf life of sliced mango fruit. *Journal of Food Engineering* **2007**, *78*, 225-229, https://doi.org/10.1016/j.jfoodeng.2005.09.022.
41. García, M. *et al.* Edible Coating as an Oil Barrier or Active System. *In: Gutiérrez-López, G.F., Barbosa-Cánovas, G.V., Welti-Chanes, J., Parada-Arias, E. (eds) Food Engineering: Integrated Approaches. Food Engineering series* **2008**, Springer, New York, NY, https://doi.org/10.1007/978-0-387-75430-7_12.
42. Aydinli, M.; Tutas, M. Water Sorption and Water Vapour Permeability Properties of Polysaccharide (Locust Bean Gum) Based Edible Films. *LWT - Food Science and Technology* **2000**, *33*, 63-67, https://doi.org/10.1006/fstl.1999.0617.
43. Garciaochoa, F.; Casas, J.A. Viscosity of Locust Bean (*Ceratonia Siliqua*) Gum Solutions. *Journal of the Science of Food and Agriculture* **1992**, *59*, 97-100, https://doi.org/10.1002/jsfa.2740590114.
44. Pinho, G.P.; Matoso, J.R.M.; Silverio, F.O.; Mota, W.C.; Lopes, P.S.N.; Ribeiro, L.M. A New Spectrophotometric Method for Determining the Enzymatic Activity of endo-beta-mannanase in Seeds. *Journal of the Brazilian Chemical Society* **2014**, *25*, 1246-1252, http://dx.doi.org/10.5935/0103-5053.20140102.
45. Guven, M.; Karaca, O.B.; Kacar, A. The effects of the combined use of stabilizers containing locust bean gum and of the storage time on Kahramanmaras-type ice creams. *International Journal of Dairy Technology* **2003**, *56*, 223-228, https://doi.org/10.1046/j.1471-0307.2003.00108.x.
46. Perrechil, F.A.; Cunha, R.L. Oil-in-water emulsions stabilized by sodium caseinate: Influence of pH, high-pressure homogenization and locust bean gum addition. *Journal of Food Engineering* **2010**, *97*, 441-448, https://doi.org/10.1016/j.jfoodeng.2009.10.041.
47. Mostafavi, F.S.; Kadkhodaee, R.; Emadzadeh, B.; Koocheki, A. Preparation and characterization of tragacanth-locust bean gum edible blend films. *Carbohydr Polym* **2016**, *139*, 20-27, https://doi.org/10.1016/j.carbpol.2015.11.069.
48. Barak, S.; Mudgil, D. Locust bean gum: processing, properties and food applications--a review. *Int J Biol Macromol* **2014**, *66*, 74-80, https://doi.org/10.1016/j.ijbiomac.2014.02.017.
49. Rojas-Argudo, C.; del Rio, M.A.; Perez-Gago, M.B. Development and optimization of locust bean gum (LBG)-based edible coatings for postharvest storage of 'Fortune' mandarins. *Postharvest Biology and Technology* **2009**, *52*, 227-234, https://doi.org/10.1016/j.postharvbio.2008.11.005.
50. Matar, G.H.; Andac, M. Antibacterial efficiency of silver nanoparticles-loaded locust bean gum/polyvinyl alcohol hydrogels. *Polymer Bulletin* **2021**, *78*, 6095-6113, https://doi.org/10.1007/s00289-020-03418-7.

51. Toh, H.S.; Jurkschat, K.; Compton, R.G. The Influence of the Capping Agent on the Oxidation of Silver Nanoparticles: Nano-impacts versus Stripping Voltammetry. *Chemistry - A European Journal* **2015**, *21*, 2998-3004, https://doi.org/10.1002/chem.201406278.
52. Magaldi, S.; Mata-Essayag, S.; Hartung de Capriles, C.; Perez, C.; Colella, M.T.; Olaizola, C.; Ontiveros, Y. Well diffusion for antifungal susceptibility testing. *Int J Infect Dis* **2004**, *8*, 39-45, https://doi.org/10.1016/j.ijid.2003.03.002.
53. Ye, J.; Wang, S.; Lan, W.; Qin, W.; Liu, Y. Preparation and properties of polylactic acid-tea polyphenol-chitosan composite membranes. *Int J Biol Macromol* **2018**, *117*, 632-639, https://doi.org/10.1016/j.ijbiomac.2018.05.080.
54. Ijaz, I.; Bukhari, A.; Gilani, E. et al. Green synthesis of silver nanoparticles using different plants parts and biological organisms, characterization and antibacterial activity. *Environmental Nanotechnology, Monitoring & Management* **2022**, *18*, 100704, https://doi.org/10.1016/j.enmm.2022.100704.
55. Abdelsattar, A.S.; Gouda, S.M.; Hassan, Y.Y.; Farouk, W.M.; Makky, S.; Nasr, A.; Hakim, T.A.; El-Shibiny, A. In vitro bacteriophage-mediated synthesis of silver nanoparticles for antibacterial applications and heavy metal detection. *Materials Letters* **2022**, *318*, 132184, https://doi.org/10.1016/j.matlet.2022.132184.
56. Kocak, Y.; Oto, G.; Meydan, I.; Seckin, H.; Gur, T.; Aygun, A.; Sen, F. Assessment of therapeutic potential of silver nanoparticles synthesized by *Ferula Pseudalliacea* rech. F. plant. *Inorganic Chemistry Communications* **2022**, *140*, 109417, https://doi.org/10.1016/j.inoche.2022.109417.
57. Long, Y.; Hu, S.; Lei, P.; Li, Y. Preparation of green silver nanoparticles with high antibacterial ability using N-maleoyl chitosan and montmorillonite. *Materials Letters* **2022**, *316*, 132044, https://doi.org/10.1016/j.matlet.2022.132044.
58. Liau, S.Y.; Read, D.C.; Pugh, W.J.; Furr, J.R.; Russell, A.D. Interaction of silver nitrate with readily identifiable groups: relationship to the antibacterial action of silver ions. *Letters in Applied Microbiology* **1997**, 279–283, https://doi.org/10.1046/j.1472-765x.1997.00219.x.
59. Yan, X.; He, B.; Liu, L.; Qu, G.; Shi, J.; Hu, L.; Jiang, G. Antibacterial mechanism of silver nanoparticles in *Pseudomonas aeruginosa*: proteomics approach. *Metallomics* **2018**, *10*, 557-564, https://doi.org/10.1039/C7MT00328E.
60. Sujit Kumar Ghosh; Pal, T. Interparticle Coupling Effect on the Surface Plasmon Resonance of Gold Nanoparticles: From Theory to Applications. *Chem. Rev.* **2007**, *107*, 4797−4862, https://doi.org/10.1021/cr0680282.
61. A. Taleb; C. Petit; Pileni, M.P. Optical Properties of Self-Assembled 2D and 3D Superlattices of Silver Nanoparticles. *J. Phys. Chem. B* **1998**, *102*, 2214-2220, https://doi.org/10.1021/jp972807s.
62. Desai, R.; Mankad, V.; Gupta, S.; Jha, P. Size Distribution of Silver Nanoparticles: UV-Visible Spectroscopic Assessment. *Nanoscience and Nanotechnology Letters* **2012**, *4*, 30-34, https://doi.org/10.1166/nnl.2012.1278.
63. Lu, R.; Yang, D.; Cui, D.; Wang, Z.; Guo, L. Egg white-mediated green synthesis of silver nanoparticles with excellent biocompatibility and enhanced radiation effects on cancer cells. *Int J Nanomedicine* **2012**, *7*, 2101-2107, https://doi.org/10.2147/ijn.s29762.
64. Gopiraman, M.; Jatoi, A.W.; Hiromichi, S.; Yamaguchi, K.; Jeon, H.Y.; Chung, I.M.; Ick Soo, K. Silver coated anionic cellulose nanofiber composites for an efficient antimicrobial activity. *Carbohydr Polym* **2016**, *149*, 51-59, https://doi.org/10.1016/j.carbpol.2016.04.084.
65. Kumar, J.; Schafer, P.; Huckelhoven, R.; Langen, G.; Baltruschat, H.; Stein, E.; Nagarajan, S.; Kogel, K-H. *Bipolaris sorokiniana*, a cereal pathogen of global concern: cytological and molecular approaches towards better control‡. *Molecular Plant Pathology* **2002**, *3*, 185–195, https://doi.org/10.1046/j.1364-3703.2002.00120.x.
66. Ma, L.J.; Geiser, D.M.; Proctor, R.H.; Rooney, A.P.; O'Donnell, K.; Trail, F.; Gardiner, D.M.; Manners, J.M.; Kazan, K. *Fusarium* pathogenomics. *Annu Rev Microbiol* **2013**, *67*, 399-416, https://doi.org/10.1146/annurev-micro-092412-155650.
67. Santos, J.; Samapundo, S.; Biyikli, A.; Van Impe, J.; Akkermans, S.; Hofte, M.; Abatih, E.N.; Sant'Ana, A.S.; Devlieghere, F. Occurrence, distribution and contamination levels of heat-resistant moulds throughout the processing of pasteurized high-acid fruit products. *Int J Food Microbiol* **2018**, *281*, 72-81, https://doi.org/10.1016/j.ijfoodmicro.2018.05.019.
68. Snyder, A.B.; Worobo, R.W. The incidence and impact of microbial spoilage in the production of fruit and vegetable juices as reported by juice manufacturers. *Food Control* **2018**, *85*, 144-150, https://doi.org/10.1016/j.foodcont.2017.09.025.